ChemPubSoc Europe

DOI: 10.1002/cmdc.201500360

CHEMMEDCHEM Full Papers

Synthetic and Biological Studies of Sesquiterpene Polygodial: Activity of 9-Epipolygodial against Drug-Resistant Cancer Cells

Ramesh Dasari,[a] Annelise De Carvalho,[b] Derek C. Medellin,[a] Kelsey N. Middleton,[a] Frédéric Hague,[c] Marie N. M. Volmar,[d] Liliya V. Frolova,[e] Mateus F. Rossato,[f] Jorge J. De La Chapa,[g] Nicholas F. Dybdal-Hargreaves,[h] Akshita Pillai,[i] Véronique Mathieu,[b] Snezna Rogelj,[e] Cara B. Gonzales,[g] João B. Calixto,[f] Antonio Evidente,[j] Mathieu Gautier,[c] Gnanasekar Munirathinam,[i] Rainer Glass,[d] Patricia Burth,[k] Stephen C. Pelly,[l] Willem A. L. van Otterlo,[l] Robert Kiss,[b] and Alexander Kornienko*[a]

Polygodial, a terpenoid dialdehyde isolated from *Polygonum hydropiper* L., is a known agonist of the transient receptor potential vanilloid 1 (TRPV1). In this investigation a series of polygodial analogues were prepared and investigated for TRPV1-agonist and anticancer activities. These experiments led to the identification of 9-epipolygodial, which has antiproliferative potency significantly exceeding that of polygodial. 9-Epipolygodial was found to maintain potency against apoptosis-resistant cancer cells as well as those displaying the multidrug-resistant (MDR) phenotype. In addition, the chemical feasibility for the previously proposed mechanism of action of polygodial, involving the formation of a Paal–Knorr pyrrole with a lysine residue on the target protein, was demonstrated by the synthesis of a stable polygodial pyrrole derivative. These studies reveal rich chemical and biological properties associated with polygodial and its direct derivatives. These compounds should inspire further work in this area aimed at the development of new pharmacological agents, or the exploration of novel mechanisms of covalent modification of biological molecules with natural products.

Introduction

Polygodial (**1**, Figure 1) is a bicyclic sesquiterpene first isolated as a pungent component of the sprout of *Polygonum hydropiper* L. (*Polygonaceae*), a plant once used as a pepper substitute in Europe and still a popular condiment for sashimi in Japan.[1] It is a member of a family of more than 80 terpenoids containing an α,β-unsaturated 1,4-dialdehyde functionality; these

[a] *Dr. R. Dasari, D. C. Medellin, K. N. Middleton, Prof. A. Kornienko*
Department of Chemistry and Biochemistry
Texas State University, San Marcos, TX 78666 (USA)
E-mail: a_k76@txstate.edu

[b] *A. De Carvalho, Prof. V. Mathieu, Prof. R. Kiss*
Laboratoire de Cancérologie et de Toxicologie Expérimentale
Faculté de Pharmacie, Université Libre de Bruxelles, 1050 Brussels (Belgium)

[c] *Dr. F. Hague, Dr. M. Gautier*
Laboratoire de Physiologie Cellulaire et Moléculaire, Faculté des Sciences
Université de Picardie Jules Verne, 80000 Amiens (France)

[d] *M. N. M. Volmar, Prof. R. Glass*
Neurosurgical Research, University Clinics Munich
Marchioninistr. 15, 81377 Munich (Germany)

[e] *Prof. L. V. Frolova, Prof. S. Rogelj*
Departments of Chemistry and Biology
New Mexico Institute of Mining and Technology
801 Leroy Place, Socorro, NM 87801 (USA)

[f] *Dr. M. F. Rossato, Prof. J. B. Calixto*
Center of Innovation and Preclinical Studies
Av. Luiz Boiteux Piazza 1302, Cachoeira do Bom Jesus
Florianópolis, SC 88056-000 (Brazil)
and
Department of Pharmacology
Federal University of Santa Catarina, Florianópolis, SC (Brazil)

[g] *J. J. De La Chapa, Prof. C. B. Gonzales*
Department of Comprehensive Dentistry
Cancer Therapy and Research Center
University of Texas Health Science Center at San Antonio
San Antonio, TX 78229 (USA)

[h] *N. F. Dybdal-Hargreaves*
Department of Pharmacology
University of Texas Health Science Center at San Antonio
San Antonio, TX 78229 (USA)

[i] *A. Pillai, Dr. G. Munirathinam*
Department of Biomedical Sciences, College of Medicine
University of Illinois, 1601 Parkview Ave., Rockford, IL 61107 (USA)

[j] *Prof. A. Evidente*
Dipartimento di Scienze Chimiche, Università di Napoli Federico II
Complesso Universitario Monte Sant'Angelo
Via Cintia 4, 80126 Napoli (Italy)

[k] *Prof. P. Burth*
Departamento de Biologia Celular e Molecular
Instituto de Biologia, Universidade Federal Fluminense
Outeiro de São João Batista, s/n Campus do Valonguinho
Centro-Niterói, RJ 24020-140 (Brazil)

[l] *Dr. S. C. Pelly, Prof. W. A. L. van Otterlo*
Department of Chemistry and Polymer Science, Stellenbosch University
Stellenbosch, Private Bag X1, Matieland, 7602 (South Africa)

Supporting information for this article is available on the WWW under http://dx.doi.org/10.1002/cmdc.201500360.

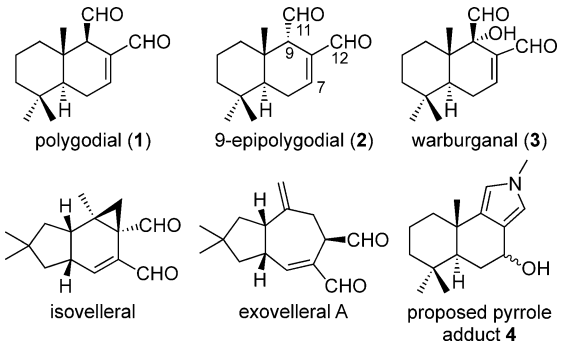

Figure 1. Structures of selected α,β-unsaturated 1,4-dialdehyde terpenoids and a proposed pyrrole adduct of **1** with methylamine (compound **4**).

compounds have been isolated from a variety of natural sources including terrestrial plants, fungi, algae, liverworts, arthropods, sponges, and mollusks.[2] Some additional members of this family are shown in Figure 1 and are believed to protect the producing organisms from predators.[2,3] Indeed, a significant number of early biological investigations involving these dialdehydes focused on their hot taste to the human tongue and antifeedant activities, both of which appeared to depend on the configuration of the aldehyde group at C9. Specifically, these studies found that polygodial (**1**) possesses potent antifeedant activity against African armyworms (*Spodoptera exempta*)[4] and fish[5] and tastes hot to the human tongue.[6] In contrast, 9-epipolygodial (**2**) is tasteless to humans and devoid of antifeedant activity toward insects[4] or fish.[5]

The antifeedant effects of polygodial and related bicyclic sesquiterpenes with a β configuration at C9 have been theorized to arise from their covalent interaction with receptors involved in taste perception. Electrophysiological studies revealed that when the maxillary palp (equivalent to taste buds) of *S. exempta* larva is repeatedly brought into contact with filter paper infused with warburganal (**3**, a related dialdehyde shown in Figure 1) the sense of taste is irreversibly blocked. As a consequence of this irreversible blockage, armyworms placed on a warburganal-treated maize leaf and subsequently transferred to an untreated leaf starve to death.[7]

The formation of covalent adducts of polygodial with biological molecules involved in taste perception has been proposed to occur through either a reaction with thiol[6] or amine[8] groups. Furthermore, based on NMR spectroscopic monitoring of the reaction of **1** with methylamine in phosphate buffer at pH 9, the formation of pyrrole adduct **4** (Figure 1) was proposed.[8–10] However, to our knowledge, no pyrrole adduct from the reaction of polygodial with primary amines has been isolated and characterized; therefore, the feasibility of such processes in chemical model systems remains to be demonstrated.

Later studies revealed anti-allergic and anti-inflammatory activities[11] associated with polygodial. Moreover, the discovery of its antifungal properties has led to its therapeutic use to control localized candidiasis (Kolorex capsules).[12] Notably, except for mild stomach discomfort and dizziness, polygodial is well tolerated by the majority of patients.[13] However, it was the discovery of polygodial's vanilloid activity and its potential use as an anti-nociceptive that has generated recent enthusiasm in the scientific literature.[13–18] In a manner similar to capsaicin, a pungent component of hot chili pepper used as a spice in the culinary traditions of many cultures, polygodial was found to inhibit the pain response invoked by formalin injection and to block acetic acid induced writhing in mice.[19] To produce their nociceptive activities, polygodial, capsaicin, and the other vanilloids are believed to target the transient receptor potential vanilloid 1 (TRPV1), a temperature-sensitive ion channel with preference for Ca^{2+} ions.[20–24] Further research has shown that in addition to its expression in sensory neurons and involvement in different modalities of pain, TRPV1 is also upregulated in various human cancer cells,[25–27] and its activation in human glioma cells leads to endoplasmic reticulum stress followed by cell death.[28] TRPV1 thus appears to be a promising target for cancer drug development, and there are many reports of studies investigating TRPV1 ligands, such as the TRPV1 agonists capsaicin[29–31] and resiniferatoxin,[27,32] as well as the TRPV1 antagonists capsazepine[29,30] and SB366791,[29] as potential anticancer agents. However, the results of mechanistic studies have complicated matters by questioning whether the anticancer effects of vanilloids are mediated by TRPV1, and have revealed that TRPV1 antagonists generally do not prevent vanilloid agonist-induced cell death.[27,29–32] Despite several reports of cytotoxic activity associated with polygodial,[33–39] to our knowledge, this TRPV1 agonist or related bicyclic sesquiterpene dialdehydes have not been investigated as potential anticancer agents. This report details our synthetic study of polygodial (**1**), the generation of a series of polygodial analogues, and the evaluation of the synthesized compounds for TRPV1 and anticancer activities. This work led to the discovery of 9-epipolygodial (**2**) as a promising agent against drug-resistant cancer and polygo-11,12-diol as a non-cytotoxic TRPV1 agonist. In addition, our study concludes that the anticancer effects of this series of compounds are also non-TRPV1-mediated, paralleling the previous findings with other TRPV1 agonists.

Results and Discussion

Chemistry

The Paal–Knorr condensation of primary amines with 1,4-dicarbonyl compounds is a well-studied classical pyrrole synthesis.[40] The biological significance of this reaction, however, appears to be severely underappreciated despite the wide occurrence of the 1,4-dicarbonyl functionality in natural products that could potentially react with lysine residues on proteins. The most well-studied example of the biological relevance of the Paal–Knorr reaction is its involvement in *n*-hexane-induced axonal atrophy in the central nervous system. It has been demonstrated both in vitro and in vivo that 2,5-hexanedione, a neurotoxic *n*-hexane metabolite, undergoes a selective Paal–Knorr condensation with lysine residues of axonal cytoskeleton proteins, forming 2,5-dimethylpyrrole adducts within specific regions of neurofilaments (Scheme 1 A).[41] To our knowledge, the

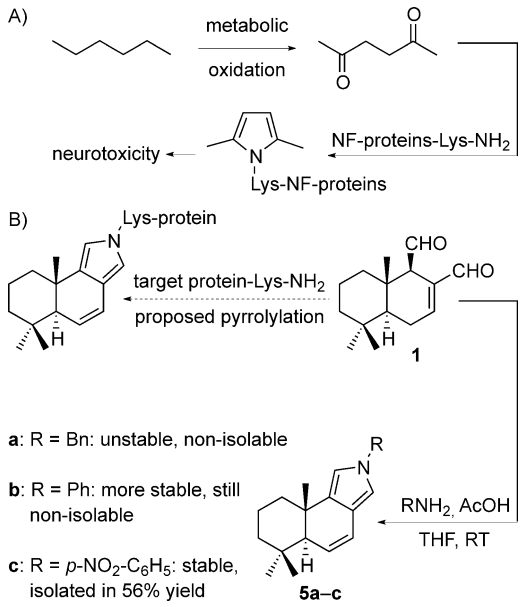

Scheme 1. A) Paal–Knorr pyrrole formation implicated in the neurotoxicity of hexane and B) proposed lysine pyrrolylation by **1** and chemical demonstration of its feasibility.

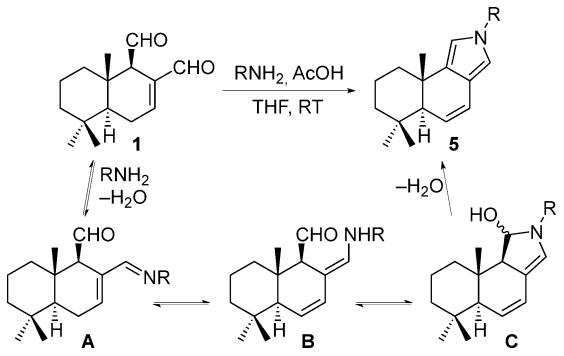

Scheme 2. Reaction mechanism of the modified Paal–Knorr pyrrole condensation of **1** with primary amines.

only other demonstrated example of lysine pyrrolylation with a 1,4-dicarbonyl compound involves lysozyme modification with spongian diterpenes, which is responsible for the Golgi-modifying properties of these marine natural products.[42]

To support the intriguing proposal that a modified Paal–Knorr condensation with a target lysine residue is responsible for the covalent interaction of polygodial with biological macromolecules as described above, compound **1** was reacted with benzyl amine under mild acid catalysis (Scheme 1B). Although TLC and MS monitoring of the reaction mixture indicated the possible formation of pyrrole **5a** (R = Bn), attempts to isolate it were unsuccessful, likely due to the susceptibility of the vinyl pyrrole functionality to oxidation. This problem was solved by using aniline and *p*-nitroaniline to make the resulting pyrrole ring system electron deficient, and in the latter case pyrrole **5c** (R = *p*-NO_2-C_6H_5) was successfully isolated as a stable polygodial derivative. Scheme 2 delineates a possible mechanism for this modified Paal–Knorr condensation, which likely involves attack by the primary amine at the more reactive C12-aldehyde to give imine **A**, which tautomerizes to dienamine **B**, eventually leading to the irreversible formation of pyrrole **5**.

Chemical derivatization of **1** included two previously described orthogonal reduction processes,[43,44] one with sodium borohydride to give polygo-11,12-diol (**6**), the other with Raney nickel to yield dihydro analogue **8**, which was present as an equilibrating mixture of dialdehyde **8a** and lactol **8b** (Scheme 3). Next, it was found that the reaction with hydrazine produced pyridazine **7**, whereas acid-catalyzed enolization/epimerization gave the C9-epimeric mixture of **1** and **2**, from which 9-epipolygodial (**2**) was isolated in 40% yield. The C12-

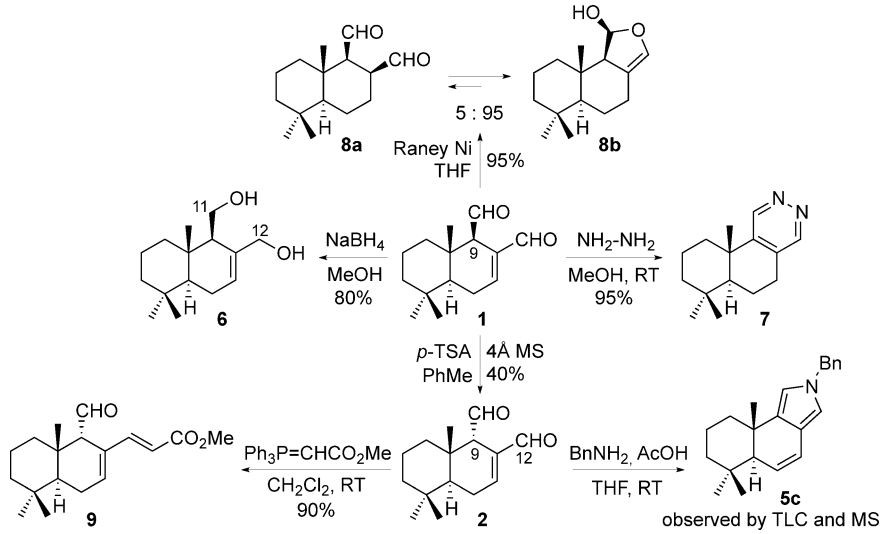

Scheme 3. General derivatization of polygodial.

aldehyde group in **2** proved to be more reactive and was selectively converted into an unsaturated ester in **9** upon a reaction with methyl (triphenylphosphoranylidene)acetate. Finally, compound **2** was found to undergo the Paal–Knorr pyrrole formation in a manner similar to epimeric **1** (Scheme 3).

Previous studies[34] also suggested that the reactive aldehyde groups in polygodial (**1**) could be masked by the formation of cyclic bis-acetals (Scheme 4). Indeed, when **1** was treated with various alcohols in the presence of *p*-toluenesulfonic acid, acetals **10**–**16** were produced as mixtures of two diastereomers with configurations at the C11 and C12 positions as shown for

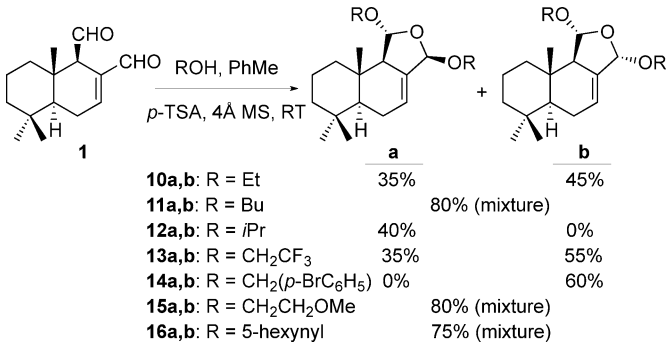

Scheme 4. Synthesis of cyclic bis-acetals **10a,b**–**16a,b**.

a and **b** (Scheme 4). The idea behind the synthesis of a series of such analogues was to facilitate the selective pyrrole formation at polygodial's target site. Although aldehyde-containing compounds do not present any particular metabolic concerns and are often present in clinical drugs (e.g., orally bioavailable male contraceptive gossypol, a dialdehyde also currently studied in cancer clinical trials[45]), moderating the reactivity of the dialdehyde functionality could be an attractive tool to improve the pharmacokinetic properties of such compounds. Indeed, with the right reactivity–stability balance of such cyclic bis-acetals, the pyrrole formation at the target protein's active site would still be possible, yet the wasteful nonspecific reactions with endogenous free amines and accessible lysine residues on abundant proteins could be minimized.

Antiproliferative activities

The synthesized compounds were evaluated for in vitro growth inhibition using the colorimetric MTT assay against a panel of five cancer cell lines including apoptosis-resistant human glioblastoma (GBM) U373,[46] human A549 non-small-cell lung cancer (NSCLC),[47] and human SKMEL-28 melanoma,[48] as well as apoptosis-sensitive human Hs683 anaplastic oligodendroglioma[46] and human MCF7 breast cancer.[49] Analysis of these data reveals that polygodial (**1**) and most of the synthesized derivatives displayed little activity in this cancer cell line panel, with the exception of 9-epipolygodial (**2**). Compound **2** was at least 20-fold more potent than polygodial **1** and did not appear to discriminate between apoptosis-resistant and apoptosis-sensitive cells by displaying similar single-digit micromolar potencies in both cell types (Table 1). Notably, the potent activity of compound **2** was initially surprising given its recent evaluation against a panel of cancer cell lines by Montenegro et al., who reported no activity associated with this compound up to 200 μM.[39] However, we retested this compound using multiple repeats with different assays across a large number of different cell lines, as can be seen below, and thus we are confident in our conclusions.

Our experience in working with cells that are intrinsically resistant to various pro-apoptotic stimuli shows that common chemotherapeutic agents that work by induction of apoptosis rapidly eliminate a certain population of sensitive cells, thus generating low GI_{50} values. However, these high potencies can be misleading, as the remaining cells can resist the effects of chemotherapeutic agents even at concentrations 100- or 1000-fold higher than their GI_{50} values.[46,50] It was thus instructive to learn that compound **2** eliminates all cells in the cultures and generates no resistant populations (close to 0% cell viability) at concentrations just slightly exceeding its GI_{50} values (Figure 2A). The contrasting effects on cell viability between **2** and the chemotherapeutic agents paclitaxel and podophyllotoxin are shown in Figure 2B and 2C. As can be seen, paclitaxel and podophyllotoxin have no effect on the proliferation of ~50% of cells in U87 GBM and A549 NSCLC cell cultures at concentrations up to 50 μM, whereas **2** exhibited potent growth inhibitory properties against most of the cells in these cultures, and, with increasing concentration, rapidly reached the antiproliferative levels of an indiscriminate cytotoxic agent, phenyl arsine oxide (PAO). Compound **2** demonstrated similar behavior in docetaxel-resistant SCC4 and cisplatin-resistant SCC25 human oral cancer cell lines, as well as docetaxel-resistant PC-3 human prostate cells (data not shown).

In contrast to the intrinsic resistance described above, tumors often initially respond to chemotherapy, but eventually become refractory to continued treatment. In such an instance of acquired resistance, cancer cells usually develop a multidrug-resistant (MDR) phenotype, affecting a broad spectrum of structurally and mechanistically diverse antitumor agents.[51,52] The phenomenon of MDR has plagued conventional therapy with vinca alkaloids,[52] for example, or taxanes,[53] and it was therefore of interest to evaluate **2** against MDR cells. The MDR uterine sarcoma cell line MES-SA/Dx5 is resistant to multiple functionally and structurally unrelated molecules,[54] and it was established by growing the parent uterine sarcoma MES-SA

Table 1. In vitro growth inhibitory effects of polygodial derivatives.

Compd	GI_{50} [μM][a]					
	A549	SKMEL-28	MCF7	U373	Hs683	Mean
1	84±9	65±3	75±2	99±6	95±1	84±6
2	6±0.1	3±0.1	2±0.1	5±0.2	6±0.2	4±1
5	98±2	>100	66±3	>100	82±2	>89±7
6	>100	>100	93±3	>100	>100	>99±1
7	>100	>100	72±3	>100	93±2	>93±5
8	35±1	72±1	25±1	86±3	33±1	50±12
9	29±1	70±1	28±1	39±1	33±0.5	40±8
10a	96±3	77±2	77±2	84±2	88±3	84±4
10b	64±2	30±1	38±3	29±1	56±2	43±7
11a,b	28±1	56±2	39±2	42±1	30±0.3	39±5
12a	>100	>100	81±3	>100	83±2	>93±4
13a	>100	>100	83±3	>100	78±4	>92±5
13b	>100	>100	66±3	>100	97±4	>93±7
14b	>100	>100	>100	>100	>100	>100
15a,b	69±4	11±1	33±1	22±3	35±2	34±10
16a,b	41±1	49±3	34±1	41±1	28±1	38±3

[a] Concentration required to decrease cell viability by 50% relative to control after 72 h treatment with the indicated compounds as determined by MTT assay; values are the mean ± SEM of sextuplicates of each experiment, performed once.

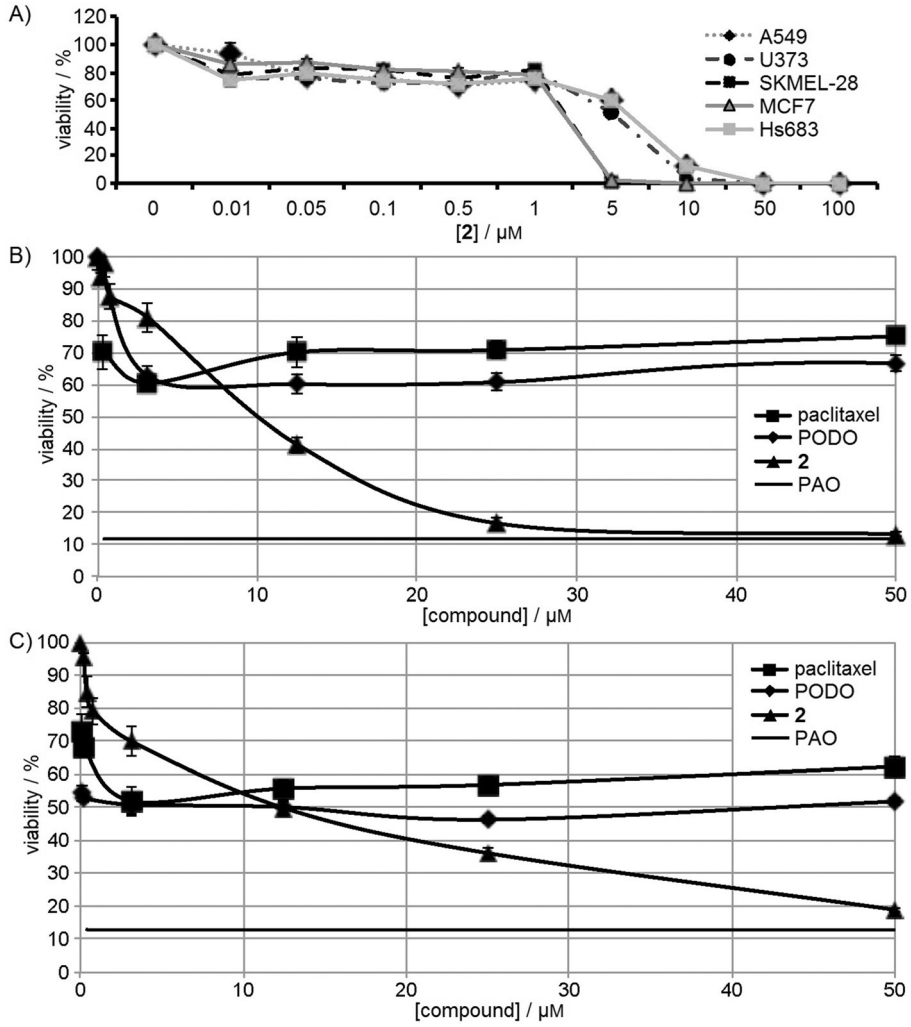

Figure 2. A) Elimination of all cells in all five cultures tested with analogue **2**, and contrasting effects on the viability of all cells between **2** and standard chemotherapeutic agents paclitaxel and podophyllotoxin (PODO) in B) U87 GBM and C) A549 NSCLC cell cultures.

cell line in the presence of increasing concentrations of doxorubicin. Paclitaxel (Table 2) and vinblastine lost their potency by 1000-fold when tested for antiproliferative activity against the MDR cell line relative to the parent line. In contrast, there was little variation in the sensitivities of the two cell lines toward **2** (Table 2).

The ability of **2** to overcome drug resistance was further evaluated using glioma cell cultures maintained under neurosphere conditions known to promote the growth of stem-like cells from human glioma tissue. Neurospheres have been shown to recapitulate human gliomas on both histological and genetic levels more faithfully than serum-cultured glioma cell lines when injected into the brains of mice,[55–58] and they are generally resistant to radiation and chemotherapy.[59–62] The small neurosphere cell culture panel chosen for this study included cells carrying a tumor-suppressor cyclin-dependent kinase inhibitor 2A (*cdkn2a*) deletion[63] as well as epidermal growth factor receptor variant III (EGFRvIII)[64] and platelet-derived growth factor subunit (PDGFB)[65] amplifications, representing frequent mutations in high-grade astrocytic tumors. The data shown in Figure 3 indicate that compound **2** used at 4 μM (average GI_{50} in Table 1) is as toxic to these cells as cannabidiol (CBD) at 10 μM, an orphan drug advanced to phase II clinical trials for the treatment of GBM.

Table 2. Antiproliferative effects of **2** against MDR cells.

Compd	GI_{50} [μM][a]	
	MES-SA	MES-SA/Dx5
paclitaxel	0.007 ± 0.001	9.8 ± 0.3
vinblastine	0.006 ± 1	5.0 ± 1.4
2	10.7 ± 0.7	6.8 ± 0.4

[a] Concentration required to decrease cell viability by 50% relative to DMSO control after 48 h treatment with the indicated compounds as determined by MTT assay; values are the mean ± SD of two independent experiments, each performed in four replicates.

Vanilloid activities

To evaluate the affinities of the synthesized polygodial derivatives for the vanilloid site of TRPV1, the compounds were assessed for their inhibition of specific binding of [^{3}H]resiniferatoxin (RTX) in rat spinal cord membranes.[16] The results (Figure 4) demonstrate that at 10 μM, polygodial (**1**) displayed 76% inhibition, whereas polygo-11,12-diol (**6**), 7,8-dihydropolygodial (**8**), and unsaturated ester **9** turned out to be more potent in this assay and showed 94, 97, and 93% inhibition, respectively. The lack of activity of 9-epipolygodial (**2**), the most promising analogue active against drug-resistant cancer, was initially surprising. However, this result is consistent with earlier findings that this natural product is tasteless to humans and devoid of antifeedant activity,[3,4] strongly suggesting that the biological effects of **2** are not mediated by TRPV1.

In a complementary assessment of TRPV1 activities, measurements of Ca^{2+} entry into MDA-MB-231 breast cancer cells abundantly expressing TRPV1 receptors[66] were performed (Figure 5). In a manner similar to capsaicin (Figure 5A), polygodial (**1**) at its average GI_{50} concentration of 80 μM (from Table 1) caused $[Ca^{2+}]_i$ increase in these assays (Figure 5B). This activity was completely inhibited with the selective TRPV1

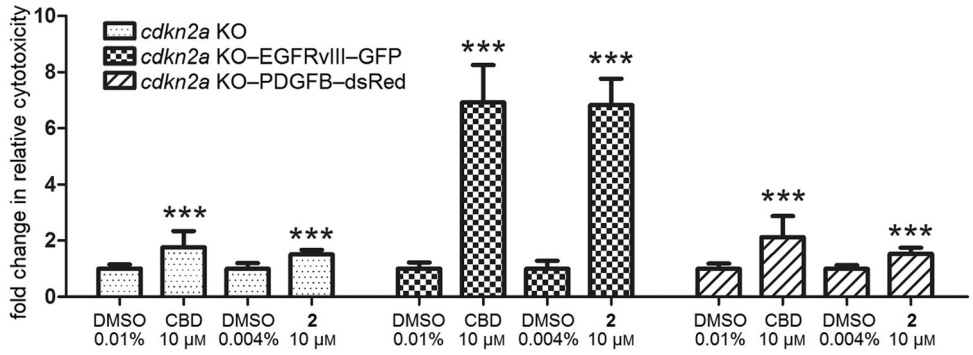

Figure 3. Activity of **2** against neurosphere glioma cell cultures with clinically relevant mutations. Transgenic mouse gliomas of defined molecular subtypes were generated by forced expression of EGFRvIII (classical GBM subtype, reporter: green fluorescent protein) or PDGFB (proneural GBM subtype, reporter: dsRed) in *cdkn2a*-deficient sub-ventricular neural precursors (NPC). These two different mouse gliomas and *cdkn2a*-deficient NPC were treated for 24 h either with 10 μM CBD versus a corresponding vehicle control (containing 0.01% DMSO) or compound **2** at 4 μM versus vehicle control (0.004% DMSO). Cytotoxicity was measured 24 h after incubation, and baseline cytotoxicity levels in the controls were arbitrarily defined as 1. Readouts from treated cells were normalized to their respective vehicle controls, and the fold change in relative cytotoxicity was calculated. Each bar represents the mean ± SD; statistical significance, as determined by unpaired *t*-tests, is indicated: ***$p < 0.001$.

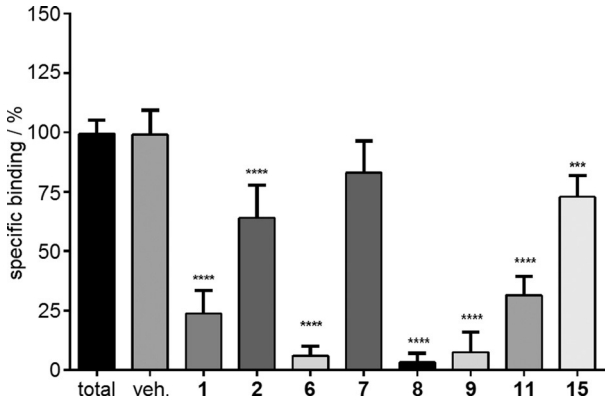

Figure 4. Evaluation of selected polygodial analogues in a [^{3}H]RTX TRPV1 displacement assay. Effect of a single concentration (10 μM) of the selected analogues in the specific binding of [^{3}H]RTX to the vanilloid site of TRPV1 receptor from rat spinal cord membranes. Results are expressed as the mean ± SEM from three independent experiments, analyzed by one-way analysis of variance (ANOVA), followed by Dunnett's multiple comparison test (***$p < 0.05$, ****$p < 0.001$).

antagonist capsazepine (Figure 5D). Furthermore, TRPV1-like currents were recorded using whole-cell patch-clamp in MDA-MB-231 cells following external perfusion with polygodial at 80 μM (Figure 5C). Taken together, these results showed that polygodial activated TRPV1 in the plasma membrane of MDA-MB-231 cells. Moreover, an MTT assay using a 24 h nontoxic treatment with capsazepine (5 μM) was performed to inhibit the activity of TRPV1 in the presence of polygodial (80 μM). The results indicate that capsazepine alone does not affect the viability of MDA-MB-231 cells, whereas polygodial strongly inhibits MDA-MB-231 viability. Interestingly, capsazepine did not counterbalance the effect of polygodial, suggesting that the anticancer effects of polygodial are also independent of TRPV1 activity (Figure 5E).

The results of the measurements of $[Ca^{2+}]_i$ into MDA-MB-231 breast cancer cells induced by 9-epipolygodial (**2**) and polygo-11,12-diol (**6**) were also consistent with the findings in the above-described [^{3}H]RTX displacement assay. Compound **2** had no effect on $[Ca^{2+}]_i$ (Figure 6A), while killing approximately half the cells at the same concentration of 4 μM (Figure 6B), clearly through a TRPV1-independent mechanism. In contrast, compound **6**, while lacking any toxicity (Figure 6D), led to a rapid increase in $[Ca^{2+}]_i$ (Figure 6C) in a TRPV1-dependent manner, as confirmed by the inhibition of this process with the TRPV1-specific antagonist capsazepine (Figure 6C).

Previous studies of the anticancer effects associated with TRPV1-targeting agents question whether these are genuinely mediated by TRPV1. Indeed, it is puzzling why both TRPV1 agonists[29–32] and antagonists[29,30] administered independently would exert antiproliferative effects against cancer cells through similar cell-death mechanisms.[29,67] It remains to be established whether there are additional functionally different intracellular targets that possess structural binding requirements similar to those at the vanilloid site on TRPV1. For example, vanilloids have indeed been shown to serve as ligands for cannabinoid receptors,[68] and both TRPV1 agonists and antagonists were found to inhibit mitochondrial function by concentration-dependent decreases in oxygen consumption and mitochondrial membrane potential.[29] Thus, structural modifications of polygodial may have dissimilar effects on TRPV1 versus this alternative hypothetical target genuinely responsible for cancer cell death. This is supported by the results of the present work with the identification of compound **2**, which, compared with polygodial, has significantly improved antiproliferative properties and yet lacks any effects on TRPV1, and compound **6**, which appears to have TRPV1-agonistic properties superior to those of polygodial while lacking any antiproliferative effects.

Computer modeling

In a search for a theoretical explanation of the experimental results obtained in this investigation, the likely binding modes of polygodial (**1**) and polygo-11,12-diol (**6**) were examined by using the cryo-EM derived structure of TRPV1 (PDB ID: 3J5R).[69] These cryo-EM studies clearly identified the binding pocket of capsaicin and RTX, thereby allowing for molecular modeling studies to probe this region for the likely binding conformations of **1** and **6**. Visual inspection of the binding pocket revealed a polar "southern region" providing possible hydrogen

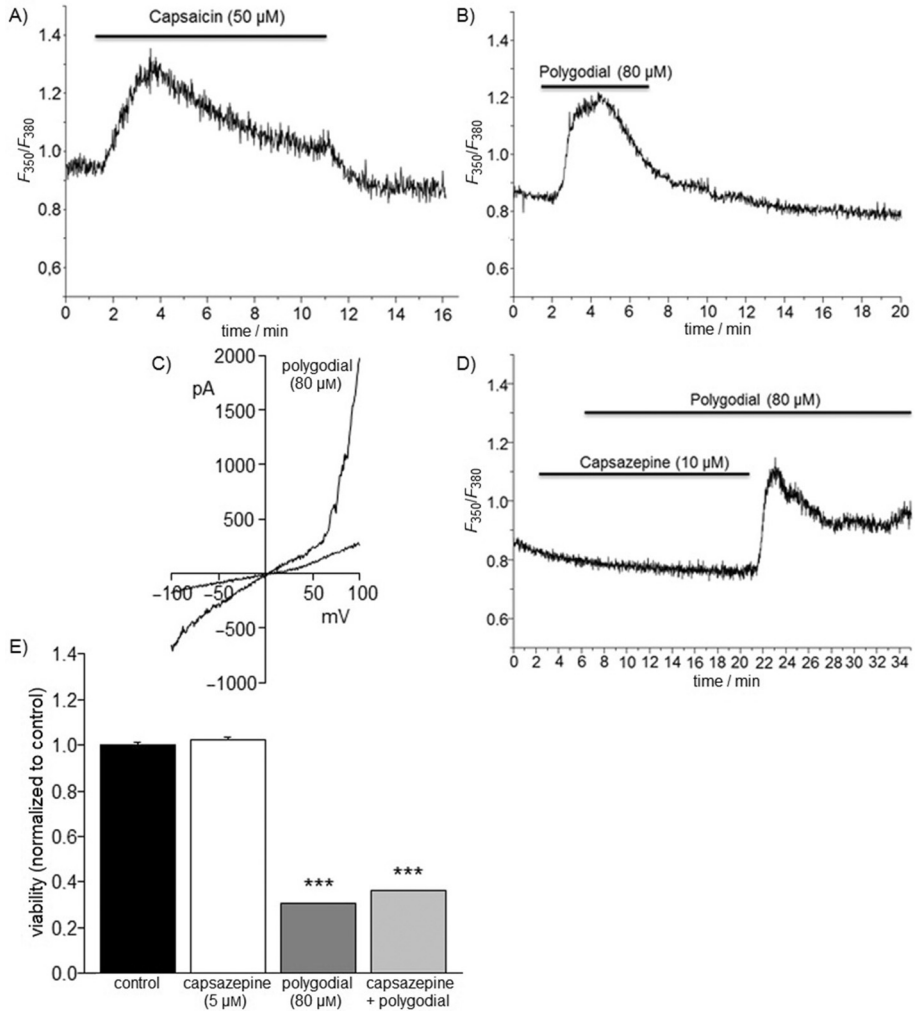

Figure 5. Effect of polygodial on TRPV1 activity in MDA-MB-231 breast cancer cells. A) Effect of capsaicin on MDA-MB-231 $[Ca^{2+}]_i$. B) Effect of polygodial on MDA-MB-231 $[Ca^{2+}]_i$. C) TRPV1-like current activation. D) Effect of capsazepine on polygodial-mediated $[Ca^{2+}]_i$ response. E) Effect of co-treatment with polygodial and capsazepine on 24 h cell viability (***$p < 0.001$; two-way ANOVA followed by Holm–Sidak tests).

bonding interactions with the side chains of Tyr511 and Thr550, while the "northern region" of the pocket is predominantly apolar (Figure 7A). Initial docking studies of **1** and **6** suggested that the preferred orientation of the ligands was indeed to facilitate hydrogen bonding to the side chains of Tyr511 and Thr550, via the carbonyl and hydroxy groups of **1** and **6**, respectively. Moreover, the hydrophobic regions of **1** and **6** were orientated toward the northern hydrophobic region of the pocket. However, visual critique of the binding mode suggested that for both **1** and **6**, the binding poses are suboptimal, with large parts of the molecules' hydrophobic portions not well accommodated within the capsaicin binding pocket. Given the poor resolution of the TRPV1 structure, optimization of the binding pocket was warranted, and to this end **1** was manually manipulated to a better fit within the pocket (by visual inspection), and the TRPV1–polygodial structure was subjected to minimization by using fixed-atom constraints of the protein backbone (not including residues within 7 Å of **1**) and a generalized Born implicit solvation model. The resulting TRPV1 structure exhibited an RMSD of 0.66 Å (residues within the binding pocket) from the original structure. Docking of **1** and **6** into the refined TRPV1 structure resulted in more sensible poses given the nature of the binding pocket, and provided an explanation for the measured binding affinities for the two structures. In the case of **1** (Figure 7B), the compound is well accommodated in the capsaicin pocket, with the aldehyde functionalities orientated toward the southern more polar region of the pocket. Hydrogen bonding is observed for the aldehyde functionalities to the side chains of Tyr511 and Thr550, with the latter serving as hydrogen bond donors. In addition, the hydrophobic portion of **1** is accommodated in the northern apolar region of the pocket. Of interest is the fact that located at the southernmost point of the binding pocket is a lysine residue Lys571 (Figure 7A). Although the side chain of this residue is not oriented toward the binding pocket, its close proximity to the aldehyde functionalities of **1** (≈10 Å) may explain the observed irreversible binding. The predicted binding pose for diol **6** differs from that of **1** in that the two hydroxy functionalities can behave as either hydrogen bond donors or acceptors (Figure 7C). For the hydrogen bonding interaction with the side chain of Tyr511 this is of no consequence, but regarding the hydrogen bonding to Thr550, it is here where the significantly stronger measured binding of **6** (relative to **1**) to TRPV1 might be explained. In the case of **1**, in order to facilitate double hydrogen bonding interactions, the side chains of both Tyr511 and Thr550 must act as donors. However, in the case of Thr550, in the apo form of the protein, this hydroxy side chain forms a hydrogen bond to the amide carbonyl group of Ala546. To form a hydrogen bond to the carbonyl group of **1**, the hydrogen bond to Ala546 must be sacrificed. However, in the case of diol **6**, the hydrogen bond between Thr550 and Ala546 need not be undone, as **6** may form a hydrogen bond with the hydroxy group of Thr550, as a hydrogen bond donor. Docking of 9-epipolygodial (**2**) interestingly revealed that inversion of stereochemistry at C9 results in a pose incapable of facilitating both hydrogen bonding interactions. Hydrogen bonding only to the less preferred Thr550 (as donor) was observed, and this may explain the substantially decreased TRPV1 activity.

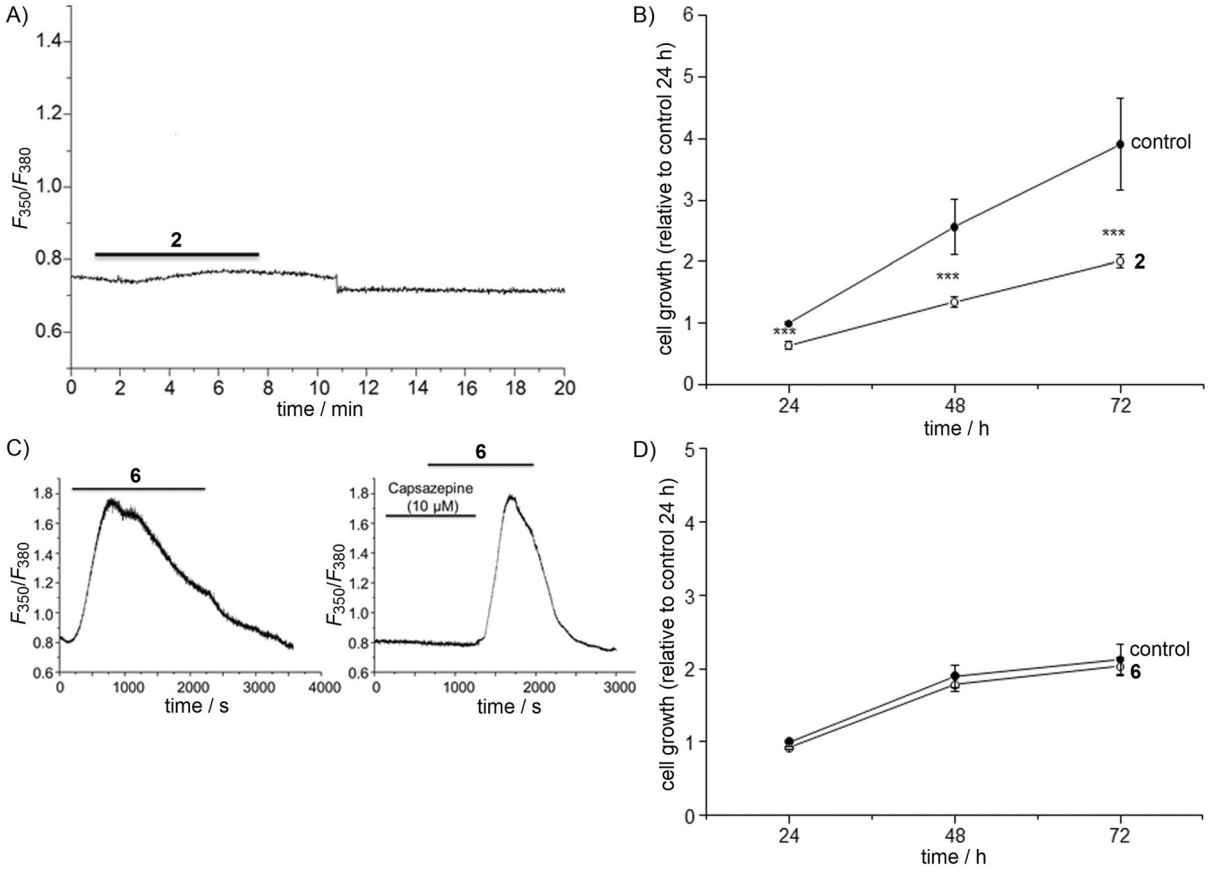

Figure 6. A) Lack of an effect of 9-epipolygodial (**2**) on $[Ca^{2+}]_i$ despite B) a pronounced effect on the viability of MDA-MB-231 breast cancer cells at 4 μM. C) Effect of polygo-11,12-diol (**6**) on $[Ca^{2+}]_i$ into TRPV1-expressing MDA-MB-231 breast cancer cells, which is blocked with capsazepine. D) Lack of an effect of polygo-11,12-diol (**6**) on cell viability at these concentrations.

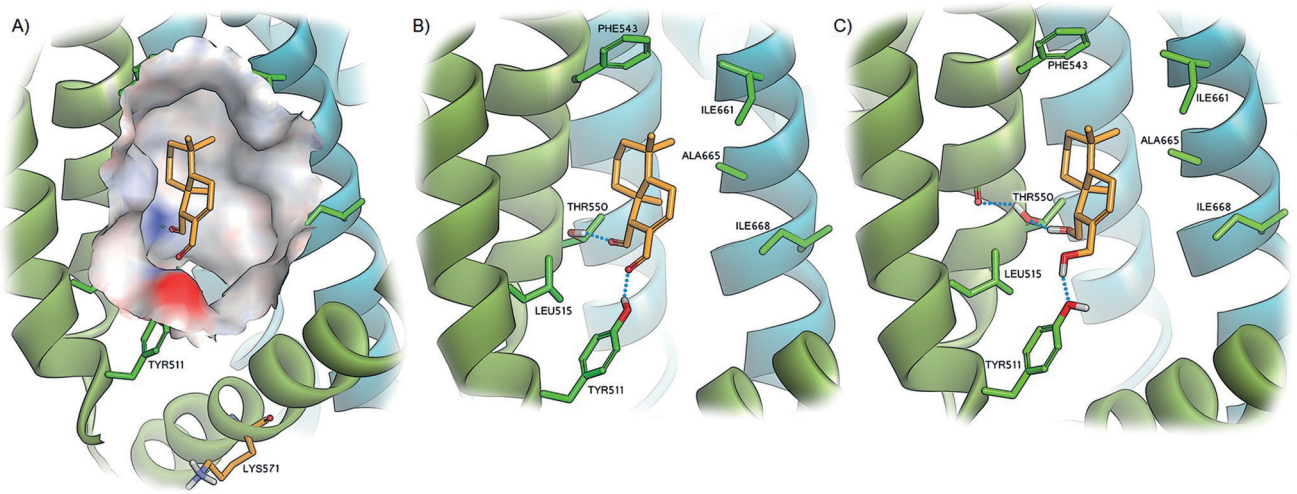

Figure 7. Molecular modeling showing the capsaicin binding region of TRPV1 with a solvent-interpolated charge surface containing A) docked polygodial (**1**) and the close proximity of Lys571. B) Hydrogen bonding interactions to Tyr511 and Thr550 are observed for docked **1**. C) Polygo-11,12-diol (**6**) docked within the pocket assumes a similar pose; however, the ability to act as a hydrogen bond donor to Thr550 means that this residue can maintain its structural hydrogen bonding interaction with Ala546.

Conclusions

Despite a safety concern involving potential tissue damage or haptenization of proteins eliciting an immune response, covalent drugs have been approved as treatments for diverse clinical applications and have had a major impact on human health.[70–72] For example, an estimated 80 billion tablets of aspirin are consumed annually in the United States, and a number of blockbuster drugs such as clopidogrel, lansoprazole, and esomeprazole are covalent inhibitors.[72] Furthermore,

covalent inhibitors are of key importance in the treatment of cancer and may be more effective in eradicating drug-resistant tumor cells.[73] Thus, mutations in the binding site of a drug target represent an important cancer cell resistance mechanism, and it has been noted that irreversible inhibitors maintain activity against such mutations caused by treatment with reversible inhibitors.[73] In one experimental confirmation of this proposal, treatment of NSCLC patients with reversible epidermal growth factor receptor (EGFR) inhibitors produced a good initial response but then led to relapse in ~50% of patients due to the development of resistance involving the expression of EGFR with mutations at T790M and/or L858R in the ATP binding site.[73,74] The NSCLC cell line harboring the T790M-L858R double-mutant form of EGFR was not affected by a panel of reversible inhibitors, but was, by contrast, significantly affected by irreversible inhibitors.[73,75] The effectiveness of irreversible inhibitors against resistant mutants may lie in the fact that mutations generally only affect the rate of covalent complex formation, and given sufficient exposure time, even mutated protein targets that react considerably more slowly will become irreversibly inactivated.[72]

The present work has led to the identification of 9-epipolygodial, an analogue of the widely studied polygodial, which is more potent than the latter by a factor of 20 against all cancer cells in the panel used in this work. Encouragingly, this compound retained activity against a significant number of drug-resistant cell lines with which it was challenged. Furthermore, the experimental results in our chemical system point to the fact that this compound likely works by covalent inhibition of its anticancer target through formation of a pyrrole adduct with a lysine residue. Such mode of reactivity in covalent target inhibition is greatly understudied. It is likely, however, that this type of reactivity toward a lysine residue over the common imine formation, may lead to greater selectivity for the target site, and thus decreased off-target effects. Indeed, a more complex chemical mechanism of the Paal–Knorr pyrrole condensation over the simple imine formation may be possible only at select protein binding sites capable of catalyzing this multistep transformation. In support of this reasoning, polygodial's therapeutic application to control *Candida albicans* infections is well tolerated by most patients.[13]

Finally, this work also resulted in the discovery of nontoxic TRPV1 agonists such as polygo-11,12-diol. Given the considerable interest in the medicinal chemistry community toward the exploitation of TRPV1-targeting agents as anti-nociceptives[14–18,21–24] and the cytotoxicity associated with some of the studied compounds,[27–32] these findings could be significant.

Experimental Section

General: All reagents, solvents, and catalysts were purchased from commercial sources (Acros Organics and Sigma–Aldrich) and used without purification. All reactions were performed in oven-dried flasks open to the atmosphere or under nitrogen or argon and monitored by thin-layer chromatography (TLC) on TLC pre-coated (250 μm) silica gel 60 F_{254} glass-backed plates (EMD Chemicals Inc.). Visualization was accomplished with UV light, iodine, and *p*-anisaldehyde stains. ^{1}H and ^{13}C NMR spectra were recorded on a Bruker 400 spectrometer. Chemical shifts (δ) are reported in ppm relative to the TMS internal standard. Abbreviations are as follows: s (singlet), d (doublet), t (triplet), q (quartet), m (multiplet). The synthesized compounds are at least 95% pure according to an HPLC–MS analysis. Polygodial (**1**) was purchased from VWR.

Compound 2: To a solution of **1** (3 mg, 0.0128 mmol) in dry toluene (1.5 mL) were added 4 Å molecular sieves and *p*-toluenesulfonic acid (cat.). The mixture was stirred at room temperature for 40 h. Solid $NaHCO_3$ was added to the reaction mixture and stirred for 10 min, filtered, and the filtrate was concentrated under reduced pressure. The crude product was purified by preparative TLC (8:92 EtOAc/hexanes) to obtain 1.2 mg of **2** as a colorless oil (40% yield); ^{1}H NMR (400 MHz, C_6D_6): δ = 9.69 (d, J = 2.4 Hz, 1H), 9.19 (s, 1H), 6.20 (dd, J = 4.9, 2.4 Hz, 1H), 1.96–1.88 (m, 1H), 1.62–1.51 (m, 1H), 1.45–1.39 (m, 2H), 1.34–1.25 (m, 2H), 1.20–1.12 (m, 2H), 0.96–0.87 (m, 2H), 0.65 (s, 3H), 0.63 (s, 3H), 0.57 ppm (d, J = 0.7 Hz, 3H); ^{13}C NMR (100 MHz, $CDCl_3$): δ = 202.2, 192.8, 153.4, 137.4, 58.5, 44.2, 42.0, 37.7, 37.1, 32.9, 32.7, 25.5, 21.9, 21.5, 18.4 ppm; HRMS (ESI) calcd for $C_{15}H_{22}NaO_2$ [M + Na] 257.1517, found 257.1519.

Compound 5c: To a solution of **1** (3 mg, 0.0128 mmol) and 4-nitroaniline (1.9 mg, 0.014 mmol) in THF (2 mL) was added AcOH (4.3 μL, 0.077 mmol). The mixture was stirred at room temperature for 20 h. After completion of the reaction, as monitored by TLC, the reaction mixture was concentrated under reduced pressure and co-distilled with toluene. The crude product was purified by preparative TLC (15:85 EtOAc/hexanes) to obtain 2.4 mg of **5c** as a yellow viscous liquid (56% yield); ^{1}H NMR (400 MHz, $CDCl_3$): δ = 8.27 (d, J = 9.2 Hz, 2H), 7.43 (d, J = 9.2 Hz, 2H), 6.98 (d, J = 2.1 Hz, 1H), 6.79 (dd, J = 2.1, 0.7 Hz, 1H), 6.55 (dd, J = 9.4, 2.9 Hz, 1H), 5.89 (dd, J = 9.4, 2.9 Hz, 1H), 2.12 (t, J = 2.9 Hz, 1H), 2.08–2.01 (m, 1H), 1.81–1.72 (m, 1H), 1.69–1.59 (m, 4H), 1.09 (s, 3H), 1.05 (s, 3H), 0.99 ppm (s, 3H); ^{13}C NMR (100 MHz, $CDCl_3$): δ = 145.4, 139.2, 128.7 (2C), 125.6 (2C), 123.5, 120.4, 118.2, 113.3, 110.5, 100.0, 53.1, 41.3, 36.4, 33.0, 29.7, 22.3, 21.6, 18.8, 14.1 ppm; HRMS (ESI) calcd for $C_{21}H_{25}N_2O_2$ [M + H] 337.1916, found 337.1916.

Compound 6: To a solution of **1** (3 mg, 0.0128 mmol) in MeOH (2 mL) was added $NaBH_4$ (1.0 mg, 0.027 mmol). The mixture was stirred at room temperature for 2 h. After completion of the reaction, as monitored by TLC, H_2O was added to the reaction mixture and MeOH was evaporated. The reaction mixture was diluted with EtOAc, and the organic phase was washed with 1 N HCl and H_2O, dried over anhydrous Na_2SO_4, and concentrated under reduced pressure. The crude product was purified by preparative TLC (10:90 EtOAc/hexanes) to obtain 2.4 mg of **6** as a colorless oil (80% yield); ^{1}H NMR (400 MHz, $CDCl_3$): δ = 5.83–5.78 (m, 1H), 4.38–4.32 (m, 1H), 3.99 (d, J = 12.1 Hz, 1H), 3.91 (dd, J = 10.9, 2.2 Hz, 1H), 3.69 (dd, J = 10.9, 8.2 Hz, 1H), 2.86 (br s, 1H), 2.14 (br s, 1H), 2.13–2.04 (m, 1H), 2.01–1.83 (m, 2H), 1.59–1.39 (m, 3H), 1.28–1.11 (m, 4H), 0.88 (s, 3H), 0.87 (s, 3H), 0.76 ppm (s, 3H); ^{13}C NMR (100 MHz, $CDCl_3$): δ = 136.9, 127.6, 67.5, 61.5, 54.5, 49.4, 42.0, 39.3, 35.6, 33.2, 33.0, 23.6, 21.9, 18.8, 14.5 ppm; HRMS (ESI) calcd for $C_{15}H_{26}NaO_2$ [M + Na] 261.1830, found 261.1829.

Compound 7: To a solution of **1** (3 mg, 0.0128 mmol) and hydrazine hydrate (0.7 μL, 0.014 mmol) in MeOH (1 mL) were added 4 Å molecular sieves. The mixture was stirred at room temperature for 20 h. After completion of the reaction, as monitored by TLC, the reaction mixture was filtered and the filtrate was concentrated under reduced pressure. The crude product was purified by preparative TLC (4:96 MeOH/$CHCl_3$) to obtain 2.8 mg of **7** as a brown viscous liquid (95% yield); ^{1}H NMR (400 MHz, $CDCl_3$): δ = 9.02 (s, 1H), 8.84

(s, 1H), 2.99–2.90 (m, 1H), 2.82 (ddd, J=18.7, 11.1, 7.7 Hz, 1H), 2.37–2.31 (m, 1H), 2.06–1.98 (m, 1H), 1.86–1.65 (m, 3H), 1.58–1.51 (m, 1H), 1.42 (td, J=12.7, 3.9 Hz, 1H), 1.31–1.23 (m, 2H), 1.23 (d, J=0.7 Hz, 3H), 0.98 (s, 3H), 0.95 ppm (s, 3H); ^{13}C NMR (100 MHz, $CDCl_3$): δ=152.2, 148.3, 145.8, 135.8, 49.5, 41.2, 36.95, 36.4, 33.4, 33.0, 26.9, 24.2, 21.5, 18.6, 17.7 ppm; HRMS (ESI) calcd for $C_{15}H_{23}N_2$ [M+H] 231.1861, found 231.1861.

Compound 8: To a suspension of Raney nickel (21.0 mg) in H_2O was added **1** (3 mg, 0.0128 mmol) in THF (2 mL). The resultant mixture was stirred at room temperature for 20 h under hydrogen atmosphere using a balloon. After completion of the reaction, as monitored by TLC, the reaction mixture was filtered through silica pad. The bed was washed several times with Et_2O and the filtrate was concentrated under reduced pressure to obtain 2.9 mg of **8** as a colorless oil (95% yield); ^{1}H NMR (400 MHz, C_6D_6): δ=5.97 (t, J=2.1 Hz, 1H), 5.38–5.31 (m, 1H), 2.41–2.35 (m, 1H), 2.25–2.18 (m, 1H), 2.06 (s, 1H), 1.86–1.74 (m, 1H), 1.52–1.40 (m, 3H), 1.35–1.31 (m, 1H), 1.31–1.27 (m, 1H), 1.12–1.00 (m, 4H), 0.78 (s, 3H), 0.74 (s, 3H), 0.72 ppm (s, 3H); HRMS (ESI) calcd for $C_{15}H_{24}NaO_2$ [M+Na] 259.1674, found 259.1674.

Compound 9: To a solution of **2** (1 mg, 0.0043 mmol) in CH_2Cl_2 (2 mL) was added methyl (triphenylphosphoranylidene)acetate (7.1 mg, 0.0021 mmol). The mixture was stirred at room temperature for 20 h. After completion of the reaction, as monitored by TLC, the reaction mixture was filtered and the filtrate was concentrated under reduced pressure. The crude product was purified by preparative TLC (9:91 EtOAc/hexanes) to obtain 1.1 mg of **9** as a colorless oil (90% yield); ^{1}H NMR (400 MHz, C_6D_6): δ=9.33 (d, J=4.8 Hz, 1H), 7.46 (d, J=15.8 Hz, 1H), 6.16 (d, J=15.8 Hz, 1H), 5.84–5.79 (m, 1H), 3.44 (s, 3H), 2.63–2.59 (m, 1H), 1.91–1.82 (m, 1H), 1.66–1.58 (m, 1H), 1.44–1.39 (m, 2H), 1.25–1.13 (m, 5H), 0.65 (s, 6H), 0.59 ppm (d, J=0.8 Hz, 3H); ^{13}C NMR (100 MHz, C_6D_6): δ=200.3, 168.0, 146.4, 141.4, 132.6, 117.1, 62.5, 51.1, 44.4, 42.2, 37.6, 36.4, 32.9, 32.7, 25.4, 21.8, 18.7, 14.2 ppm; HRMS (ESI) calcd for $C_{18}H_{26}NaO_3$ [M+Na] 313.1780, found 313.1779.

General procedure for acetals 10–16: To a solution of **1** (3 mg, 0.0128 mmol) in dry toluene (2 mL) were added a selected alcohol (0.5 mL), 4 Å molecular sieves and *p*-toluenesulfonic acid (cat.). The resulting mixture was stirred at room temperature for 20 h. Solid $NaHCO_3$ was added and the reaction mixture was stirred for 10 min, filtered, and the filtrate was concentrated under reduced pressure. The crude product was purified by preparative TLC (8:92 EtOAc/hexanes) to obtain acetal products **10–16**.

Compound 10a: 35% yield, colorless oil; ^{1}H NMR (400 MHz, C_6D_6): δ=5.90–5.86 (m, 1H), 5.68–5.65 (m, 1H), 5.18 (d, J=6.1 Hz, 1H), 3.99–3.86 (m, 2H), 3.55–3.45 (m, 2H), 2.48–2.42 (m, 1H), 2.03–1.93 (m, 1H), 1.84–1.71 (m, 2H), 1.52–1.42 (m, 1H), 1.35–1.25 (m, 5H), 1.19 (t, J=7.2 Hz, 3H), 1.17 (t, J=7.2 Hz, 3H), 0.87 (s, 3H), 0.80 (s, 3H), 0.74 ppm (s, 3H); HRMS (ESI) calcd for $C_{19}H_{32}NaO_3$ [M+Na] 331.2249, found 331.2248.

Compound 10b: 45% yield, colorless oil; ^{1}H NMR (400 MHz, C_6D_6): δ=5.59–5.56 (m, 1H), 5.36 (s, 1H), 5.14 (d, J=4.3 Hz, 1H), 3.98–3.83 (m, 2H), 3.57–3.44 (m, 2H), 2.76–2.70 (m, 1H), 1.95–1.86 (m, 1H), 1.74–1.62 (m, 2H), 1.50–1.43 (m, 1H), 1.35–1.27 (m, 4H), 1.26–1.17 (m, 7H), 0.79 (s, 3H), 0.76 (s, 3H), 0.70 ppm (s, 3H); HRMS (ESI) calcd for $C_{19}H_{32}NaO_3$ [M+Na] 331.2249, found 331.2248.

Compounds 11a+b (1:1.5 mixture): 80% yield, colorless oil; ^{1}H NMR (400 MHz, C_6D_6): δ=5.92–5.87 (m, 1H), 5.71–5.67 (m, 1H), 5.59 (dd, J=6.8, 3.1 Hz, 1.5H), 5.39–5.37 (m, 1.5H), 5.20 (d, J=6.1 Hz, 1H), 5.15 (d, J=4.3 Hz, 1.5H), 4.03–3.86 (m, 5H), 3.56–3.43 (m, 5H), 2.78–2.71 (m, 1.5H), 2.50–2.43 (m, 1H), 2.05–1.79 (m, 5H), 1.71–1.58 (m, 12.5H), 1.54–1.39 (m, 12H), 1.39–1.22 (m, 11H), 1.19–1.13 (m, 2H), 0.95–0.85 (m, 18H), 0.81 (s, 3H), 0.80 (s, 4.5H), 0.78 (s, 4.5H), 0.75 (s, 3H), 0.71 ppm (s, 4.5H), total number of protons = 100H [40H (40H×1.0) of **11a**, 60H (40H×1.5) of **11b**]; HRMS (ESI) calcd for $C_{23}H_{40}NaO_3$ [M+Na] 387.2875, found 387.2879.

Compound 12a: 40% yield, colorless oil; ^{1}H NMR (400 MHz, C_6D_6): δ=5.88–5.84 (m, 1H), 5.73–5.70 (m, 1H), 5.27 (d, J=6.2 Hz, 1H), 4.03–3.89 (m, 2H), 2.47–2.41 (m, 1H), 2.05–1.96 (m, 1H), 1.89–1.73 (m, 2H), 1.51 (dt, J=13.3, 2.9 Hz, 1H), 1.40–1.29 (m, 11H), 1.15–1.09 (m, 6H), 0.90 (s, 3H), 0.81 (s, 3H), 0.75 ppm (s, 3H); HRMS (ESI) calcd for $C_{21}H_{36}NaO_3$ [M+Na] 359.2562, found 359.2560.

Compound 13a: 35% yield, colorless oil; ^{1}H NMR (400 MHz, C_6D_6): δ=5.74–5.70 (m, 1H), 5.34 (s, 1H), 4.90 (d, J=5.9 Hz, 1H), 3.86–3.71 (m, 2H), 3.57–3.42 (m, 2H), 2.25–2.19 (m, 1H), 1.89–1.80 (m, 1H), 1.68–1.60 (m, 2H), 1.32–1.28 (m, 2H), 1.27–1.23 (m, 2H), 1.14–1.02 (m, 2H), 0.73 (s, 3H), 0.70 (s, 3H), 0.67 ppm (s, 3H); HRMS (ESI) calcd for $C_{19}H_{26}F_6KO_3$ [M+K] 455.1423, found 455.1423.

Compound 13b: 55% yield, colorless oil; ^{1}H NMR (400 MHz, C_6D_6): δ=5.43 (dd, J=6.8, 3.1 Hz, 1H), 5.09 (s, 1H), 4.90 (d, J=4.0 Hz, 1H), 3.80–3.65 (m, 2H), 3.63–3.44 (m, 2H), 2.52–2.46 (m, 1H), 1.83–1.74 (m, 1H), 1.60–1.46 (m, 2H), 1.30–1.21 (m, 2H), 1.09–0.89 (m, 4H), 0.72 (s, 3H), 0.68 (s, 3H), 0.57 ppm (s, 3H); ^{13}C NMR (100 MHz, C_6D_6): δ=136.0, 127.4, 125.7, 122.8, 106.5, 104.0, 65.3 (d), 63.9 (d), 57.7, 49.2, 42.2, 39.3, 32.9, 32.4, 29.8, 23.6, 21.4, 18.6, 14.1 ppm; HRMS (ESI) calcd for $C_{19}H_{26}F_6KO_3$ [M+K] 455.1423, found 455.1423.

Compound 14b: 60% yield, colorless oil; ^{1}H NMR (400 MHz, C_6D_6): δ=7.29–7.24 (m, 4H), 7.06–6.97 (m, 4H), 5.57–5.52 (m, 1H), 5.34 (s, 1H), 5.15 (d, J=4.0 Hz, 1H), 4.65 (dd, J=24.7, 12.3 Hz, 2H), 4.35 (d, J=12.2 Hz, 2H), 2.78–2.72 (m, 1H), 1.98–1.86 (m, 1H), 1.72–1.61 (m, 1H), 1.46–1.38 (m, 2H), 1.22–1.10 (m, 3H), 1.10–0.96 (m, 2H), 0.78 (s, 3H), 0.73 (s, 3H), 0.69 ppm (s, 3H); HRMS (ESI) calcd for $C_{29}H_{34}Br_2NaO_3$ [M+Na] 611.0772, found 611.0791.

Compounds 15a+b (1.0:1.7 mixture): 80% yield, colorless oil; ^{1}H NMR (400 MHz, C_6D_6): δ=5.93–5.87 (m, 1H), 5.74–5.70 (m, 1H), 5.58–5.53 (m, 1.7H), 5.40 (s, 1.7H), 5.24 (d, J=6.1 Hz, 1H), 5.19 (d, J=4.2 Hz, 1.7H), 4.04–3.94 (m, 5H), 3.79–3.67 (m, 5H), 3.61–3.33 (m, 11H), 3.20 (s, 5H), 3.18 (s, 5H), 3.15 (s, 3H), 3.14 (s, 3H), 2.76–2.70 (m, 1.7H), 2.47–2.41 (m, 1H), 1.95–1.83 (m, 4H), 1.75–1.62 (m, 2H), 1.53–1.42 (m, 2H), 1.42–1.25 (m, 8H), 1.27–1.19 (m, 4H), 1.15–1.01 (m, 6H), 0.87 (s, 3H), 0.79 (s, 3H), 0.77 (s, 5H), 0.73 (s, 5H), 0.73 (s, 3H), 0.70 ppm (s, 5H), total number of protons = 97H [36H (36H×1.0) of **15a**, 61H (36H×1.7) of **15b**]; HRMS (ESI) calcd for $C_{21}H_{36}NaO_5$ [M+Na] 391.2460, found 391.2460.

Compounds 16a+b (1:1 mixture): 75% yield, colorless oil; ^{1}H NMR (400 MHz, C_6D_6): δ=5.90–5.82 (m, 1H), 5.63–5.53 (m, 2H), 5.30 (s, 1H), 5.14–5.05 (m, 2H), 3.97–3.75 (m, 4H), 3.54–3.32 (m, 4H), 2.72–2.62 (m, 1H), 2.45–2.36 (m, 1H), 2.10–1.86 (m, 8H), 1.82–1.74 (m, 4H), 1.73–1.50 (m, 16H), 1.49–1.26 (m, 8H), 1.26–0.92 (m, 10H), 0.88–0.68 ppm (m, 18H), total number of protons = 80H [40H of **16a**, 40H of **16b**]; HRMS (ESI) calcd for $C_{27}H_{40}NaO_3$ [M+Na] 435.2875, found 435.2878.

Cell culture: Human cancer cell lines were obtained from the American Type Culture Collection (ATCC; Manassas, VA, USA), the European Collection of Cell Culture (ECACC; Salisbury, UK), and the Deutsche Sammlung von Mikroorganismen und Zellkulturen (DSMZ; Braunschweig, Germany). Human mammary carcinoma MCF7 cells were cultured in RPMI-1640 medium supplemented with 10% FBS. U87 cells (ATCC HTB-14) were cultured in DMEM, whereas A549 cells (DSMZ ACC107) were cultured in RPMI-1640

medium supplemented with 10% heat-inactivated FBS. Hs683 (ATCC HTB-138) GBM cells were cultivated in RPMI-1640 medium supplemented with 10% FBS. Human uterine sarcoma MES-SA and MES-SA/Dx5 cells were cultured in RPMI-1640 medium supplemented with 10% FBS, with MES-SA/Dx5 maintained in the presence of 500 nM doxorubicin (Sigma). SKMEL-28 cells (ATCC HTB72) and U373 GBM cells (ECACC 08061901) were cultured in RPMI-1640 medium supplemented with 10% heat-inactivated FBS. Cell culture media were supplemented with 4 mM glutamine (Lonza BE17-605E), 100 $\mu g\,mL^{-1}$ gentamicin (Lonza 17-5182), and penicillin–streptomycin (200 $U\,mL^{-1}$ and 200 $\mu g\,mL^{-1}$, respectively; Lonza 17-602E). MDA-MB-231 (ATCC HTB-26) epithelial mammary adenocarcinoma cells were cultured in Eagle's minimum essential medium (EMEM, Invitrogen) containing 5% FCS (Cambrex), 2 mM L-glutamine (Invitrogen), 0.06% HEPES (Invitrogen), and penicillin (50 $IU\,mL^{-1}$)–streptomycin (50 $\mu g\,mL^{-1}$, Invitrogen) at 37 °C in a humidified atmosphere of 5% CO_2 in air. Transformed mouse NPCs were cultured in suspension under neurosphere conditions at 37 °C in a humidified atmosphere of 95% O_2 and 5% CO_2 in DMEM F-12 (Invitrogen 11320-074) supplemented with 1× B27 supplement (Invitrogen 17504-044), 5% penicillin–streptomycin (Biochrom 10378-017), 10 $ng\,mL^{-1}$ EGF (R&D systems 236-EG), and 10 $ng\,mL^{-1}$ FGF (PeproTech 100-18B).

Antiproliferative properties: The antiproliferative properties of the synthesized compounds were evaluated by MTT assay.[76–78] All compounds were dissolved in DMSO at a concentration of either 100 or 50 mM prior to cell treatment. The cells were trypsinized and seeded at various concentrations depending on cell type. Cells were grown for 24–72 h, treated with compounds at concentrations ranging from 0.001 to 100 μM and incubated for 24, 48, or 72 h in 100 or 200 μL media depending on the cell line used. The number of experiments and replicates varied depending on the cell line. Cells treated with 0.1% DMSO were used as a negative control; 1 μM PAO was used as a positive control.

Selection of doxorubicin-resistant cells: Selection of the MES-SA/Dx5 cell line was done according to Harker and Sikic.[54] The cells were split and allowed to adhere overnight. The next day cells were initially exposed to doxorubicin (DOX) at a concentration of 100 nM, which represents the GI_{50} concentration. The cells were maintained at this DOX concentration until their growth rate reached that of the untreated cells. The DOX concentration was then increased in two-fold increments following the same growth criteria at each concentration to a final DOX concentration of 500 nM. Each new DOX concentration required approximately two passages to reach the growth rate of the untreated cells.

CytoTox-Fluor cytotoxicity assays: The CytoTox-Fluor cytotoxicity assay (Promega) was used according to manufacturer's instructions. In brief, 1.5×10^4 cells per well (five replicates per condition) were plated in 24-well plates in 450 μL of culture medium (DMEM F-12 without phenol red). They then received 50 μL of culture medium supplemented with test compounds or the respective vehicle control. After 24 h incubation at 37 °C, cell suspension (20 μL) was transferred to a black 384-well plate and mixed with bis-AAF-R110 substrate dilution (20 μL). After 2 h incubation at 37 °C, the fluorescence intensity was measured using a Tecan Infinite F200 fluorescence plate reader (λ_{ex} 485 nm, λ_{em} 520 nm). Blank values were subtracted from all wells, and the fluorescence readout for untreated cells (vehicle control) was normalized to 1. Readouts from cells receiving various treatment conditions were normalized to those of untreated cells, and the fold change of relative cytotoxicity to untreated controls was calculated for each well. Outliers were detected and omitted, if any, using the Grubbs test. Graphs were generated with GraphPad Prism 5 software (version 5.01).

[^{3}H]Resiniferatoxin binding assays: To evaluate the possible affinity of different analogues to the vanilloid site of TRPV1, a [^{3}H]resiniferatoxin ([^{3}H]RTX) binding assay was performed as previously described.[79,80] Briefly, rat spinal cords were homogenized in buffer A (10 mM HEPES pH 7.4, 5 mM KCl, 5.8 mM NaCl, 2 mM $MgCl_2$, 0.75 mM $CaCl_2$, 137 mM sucrose) and centrifuged for 10 min at 1000 *g* at 4 °C, and the supernatant was further centrifuged for 30 min at 35000 *g* at 4 °C. The resulting pellets were than resuspended in buffer A and frozen until assayed. The binding reaction was performed in a final volume of 500 μL, containing buffer A (plus 0.25 $mg\,mL^{-1}$ BSA), membranes (0.5 $mg\,mL^{-1}$), and 2 nM [^{3}H]RTX in the presence or absence of polygodial analogues (10 μM). For measurements of nonspecific binding, nonradioactive RTX (100 μM) was included. The reaction was started by incubating tubes at 37 °C for 60 min and then stopped by transferring the tubes to an ice bath and adding 100 μg bovine α_1-acid glycoprotein (to decrease nonspecific binding). Finally, the bound and free membranes [^{3}H]RTX were separated by centrifugation for 30 min at 35000 *g* at 4 °C. The pellet was used to quantify the scintillation counting. Specific binding was calculated as the difference between total and nonspecific binding, and the results are reported as a percentage of specific binding.

Intracellular Ca^{2+} measurements: Cells were grown on glass coverslips for fluorescence imaging. The cytosolic calcium levels were measured using Fura-2-loaded cells. Cells were loaded for 45 min at 37 °C in a humidified atmosphere of 5% CO_2 in air with 3.3 μM Fura-2/AM prepared in saline solution. Fluorescence was excited at λ 350 and 380 nm alternately using a monochromator (Polychrome IV; TILL Photonics, Planegg, Germany), and captured by a Cool SNAP HQ camera (Princeton Instruments, France) after filtration through a long-pass filter (λ 510 nm). Metafluor software 7.0 (Molecular Devices) was used for acquisition and analysis. All recordings were carried out at room temperature. Cells were perfused with saline solutions consisting of 140 mM NaCl, 5 mM KCl, 2 mM $CaCl_2$, 2 mM $MgCl_2$, 10 mM HEPES, and 5 mM glucose (adjusted to pH 7.4 with NaOH).

Electrophysiological recordings: TRP currents were recorded using the conventional patch-clamp technique in whole-cell configuration. Briefly, the holding membrane potential was held at −40 mV, and currents were elicited by a ramp depolarization from −100 to +100 mV for 350 ms. The interval between each ramp depolarization was 10 s. The patch pipettes (3–5 MΩ) were made from hematocrit glass using a vertical puller (P30 vertical micropipette puller; Sutter Instruments). The following extracellular solution was used: 140 mM sodium gluconate, 5 mM potassium gluconate, 2 mM magnesium gluconate, 2 mM calcium gluconate, 10 mM HEPES, 5 mM glucose, and 5 mM TEA-Cl (adjusted to pH 7.4 with NaOH). The following intrapipette solution was used: 145 mM cesium gluconate, 8 mM sodium gluconate, 10 mM EGTA, 3 mM magnesium gluconate, and 10 mM HEPES (adjusted to pH 7.2 with CsOH). Signals were filtered at 1 kHz and digitized at 5 kHz using an Axopatch 200B patch-clamp amplifier (Molecular Devices, Sunnyvale, CA, USA) combined with a Digidata 1322A instrument (Molecular Devices). Electrophysiological protocols and analyses were made using pClamp 10 and Clampfit software (both by Molecular Devices), as well as Origin 6.0 (Microcal Software, Northampton, MA, USA). All experiments were performed at room temperature.

Computer modeling: Molecular modelling was performed using Discovery Studio 4.5 (DS). The receptor template was obtained from

the RCSB Protein Data Bank (PDB ID: 3J5R) and chains B and D were retained for the simulations. Protein preparation was carried out using the Prepare Protein protocol launched from within DS. All docking simulations were carried out using a modified CDocker protocol with pre-generation of ligand conformations to adequately sample conformational space. Minimizations were carried out within DS, employing the CHARMm force field (version 39.1).

Acknowledgements

This project was supported by grants from the National Institute of General Medical Sciences (P20M103451), the National Cancer Institute (CA186046-01A1), the Welch Foundation (AI-0045), and the National Science Foundation (NSF award 0946998). S.R. and L.F. acknowledge their NMT Presidential Research Support. L.F. acknowledges the National Science Foundation (NSF award IIA-1301346). R.K. is a director of research with the Fonds National de la Recherche Scientifique (FRS-FNRS, Belgium). S.C.P. and W.v.O. gratefully acknowledge support from the National Research Foundation (NRF) of South Africa, as well as Stellenbosch University. The authors are grateful to Anntherese Kornienko for her help with creating Figure 2.

Keywords: capsaicin · capsazepine · ion channels · resiniferatoxin · vanilloid

[1] A. Ohsuka, *Nippon Kagaku Zasshi* **1963**, *84*, 748 – 752.
[2] M. Jonassohn, O. Sterner, *Trends Org. Chem.* **1997**, *6*, 23 – 43.
[3] V. Caprioli, G. Cimino, R. Colle, M. Gavagnin, G. Sodano, A. Spinella, *J. Nat. Prod.* **1987**, *50*, 146 – 151.
[4] K. Nakanishi, I. Kubo, *Isr. J. Chem.* **1977**, *16*, 28 – 31.
[5] G. Cimino, S. De Rosa, S. De Stefano, G. Sodano, *Comp. Biochem. Physiol.* **1982**, *73B*, 471 – 474.
[6] I. Kubo, I. Ganjian, *Experientia* **1981**, *37*, 1063 – 1064.
[7] I. Kubo, K. Nakanishi in *Advances in Pesticide Science, Part 2* (Ed.: H. Geissbuhler), Pergamon Press, New York, **1979**, p. 284.
[8] G. Cimino, A. Spinella, G. Sodano, *Tetrahedron Lett.* **1984**, *25*, 4151 – 4152.
[9] M. D'Ischia, G. Prota, G. Sodano, *Tetrahedron Lett.* **1982**, *23*, 3295 – 3298.
[10] G. Cimino, G. Sodano, A. Spinella, *Tetrahedron* **1987**, *43*, 5401 – 5410.
[11] F. M. da Cunha, T. S. Frode, G. L. Mendes, A. Malheiros, V. C. Filho, R. A. Yunes, J. B. Calixto, *Life Sci.* **2001**, *70*, 159 – 169.
[12] S. H. Lee, J. R. Lee, C. S. Lunde, I. Kubo, *Planta Med.* **1999**, *65*, 204 – 208.
[13] O. Sterner, A. Szallasi, *Trends Pharmacol. Sci.* **1999**, *20*, 459 – 465.
[14] E. Andre, J. Ferreira, A. Malheiros, R. A. Yunes, J. B. Calixto, *Neuropharmacology* **2004**, *46*, 590 – 597.
[15] C. Della Monica, L. De Petrocellis, V. Di Marzo, R. Landi, I. Izzo, A. Spinella, *Bioorg. Med. Chem. Lett.* **2007**, *17*, 6444 – 6447.
[16] E. André, B. Campi, M. Trevisani, J. Ferreira, A. Malheiros, R. A. Yunes, J. B. Calixto, P. Geppetti, *Biochem. Pharmacol.* **2006**, *71*, 1248 – 1254.
[17] M. D'Acunto, C. D. Monica, I. Izzo, L. De Petrocellis, V. di Marzo, A. Spinella, *Tetrahedron* **2010**, *66*, 9785 – 9789.
[18] Y. Iwasaki, M. Tanabe, Y. Kayama, M. Abe, M. Kashio, K. Koizumi, Y. Okumura, Y. Morimitsu, M. Tominaga, Y. Ozawa, T. Watanabe, *Life Sci.* **2009**, *85*, 60 – 69.
[19] G. L. Mendes, A. R. Santos, M. M. Campos, K. S. Tratsk, R. A. Yunes, V. Cechinel Filho, J. B. Calixto, *Life Sci.* **1998**, *63*, 369 – 381.
[20] M. J. Caterina, M. A. Schumacher, M. Tominaga, T. A. Rosen, J. D. Levine, D. Julius, *Nature* **1997**, *389*, 816 – 824.
[21] D. Julius, A. I. Basbaum, *Nature* **2001**, *413*, 203 – 210.
[22] M. Trevisani, D. Smart, M. J. Gunthorpe, M. Tognetto, M. Barbieri, B. Campi, S. Amadesi, J. Gray, J. C. Jerman, S. J. Brough, D. G. D. Owen Smith, A. D. Randall, S. Harrison, A. Bianchi, J. B. Davis, P. Geppetti, *Nat. Neurosci.* **2002**, *5*, 546 – 551.
[23] J. B. Davis, J. Gray, M. J. Gunthorpe, J. P. Hatcher, P. T. Davey, P. Overend, M. H. Harries, J. Latcham, C. Clapham, K. Atkinson, S. A. Hughes, K. Rance, E. Grau, A. J. Harper, P. L. Pugh, D. C. Rogers, S. Bingham, A. Randall, S. A. Sheardown, *Nature* **2000**, *405*, 183 – 187.
[24] M. J. Caterina, D. Julius, *Annu. Rev. Neurosci.* **2001**, *24*, 487 – 517.
[25] L. S. Premkumar, M. Bishnoi, *Curr. Top. Med. Chem.* **2011**, *11*, 2192 – 2209.
[26] D. Gkika, N. Prevarskaya, *Biochim. Biophys. Acta.* **2009**, *1793*, 953 – 958.
[27] M. Hartel, F. F. di Mola, F. Selvaggi, G. Mascetta, M. N. Wente, K. Felix, N. A. Giese, U. Hinz, P. Di Sebastiano, M. W. Buchler, H. Friess, *Gut* **2006**, *55*, 519 – 528.
[28] K. Stock, J. Kumar, M. Synowitz, S. Petrosino, R. Imperatore, E. S. Smith, P. Wend, B. Purfürst, U. A. Nuber, U. Gurok, V. Matyash, J. H. Wälzlein, S. R. Chirasani, G. Dittmar, B. F. Cravatt, S. Momma, G. R. Lewin, A. Ligresti, L. De Petrocellis, L. Cristino, V. Di Marzo, H. Kettenmann, R. Glass, *Nat. Med.* **2012**, *18*, 1232 – 1238.
[29] A. Athanasiou, P. A. Smith, S. Vakilpour, N. M. Kumaran, A. E. Turner, D. Bagiokou, R. Layfield, D. E. Ray, A. D. Westwell, S. P. H. Alexander, D. E. Kendall, D. N. Lobo, S. A. Watson, A. Lophatanon, K. A. Muir, D. A. Guo, T. E. Bates, *Biochem. Biophys. Res. Commun.* **2007**, *354*, 50 – 55.
[30] C. B. Gonzales, N. B. Kirma, J. J. De La Chapa, R. Chen, M. A. Henry, S. Luo, K. M. Hargreaves, *Oral Oncol.* **2014**, *50*, 437 – 447.
[31] M. Skrzypski, M. Sassek, S. Abdelmessih, S. Mergler, C. Grotzinger, D. Metzke, T. Wojciechowicz, K. W. Nowak, M. Z. Strowski, *Cell. Signalling* **2014**, *26*, 41 – 48.
[32] V. Farfariello, S. Liberati, M. B. Morelli, D. Tomassoni, M. Santoni, M. Nabissi, A. Giannantoni, G. Santoni, C. Amantini, *Chem.-Biol. Interact.* **2014**, *224*, 128 – 135.
[33] N. Allouche, C. Apel, M. T. Martin, V. Dumontet, F. Guéritte, M. Litaudon, *Phytochemistry* **2009**, *70*, 546 – 553.
[34] T. Tozyo, F. Yasuda, H. Nakai, H. Tada, *J. Chem. Soc. Perkin Trans. 1* **1992**, 1859 – 1866.
[35] A. F. Barrero, M. Cortés, E. A. Manzaneda, E. Cabrera, R. Chahboun, M. Lara, A. R. Rivas, *J. Nat. Prod.* **1999**, *62*, 1488 – 1491.
[36] H. Anke, O. Sterner, *Planta Med.* **1991**, *57*, 344 – 346.
[37] A. Forsby, M. Andersson, L. Lewan, O. Sterner, *Toxicol. In Vitro* **1991**, *5*, 9 – 14.
[38] M. Andersson, F. Bocchio, O. Sterner, A. Forsby, L. Lewan, *Toxicol. In Vitro* **1993**, *7*, 1 – 6.
[39] I. Montenegro, G. Tomasoni, C. Bosio, N. Quinones, A. Madrid, H. Carrasco, A. Olea, R. Martinez, M. Cuellar, J. Villena, *Molecules* **2014**, *19*, 18993 – 19006.
[40] V. Amarnath, D. C. Anthony, K. Amarnath, W. M. Valentine, L. A. Wetterau, D. G. Graham, *J. Org. Chem.* **1991**, *56*, 6924 – 6931.
[41] L. Zhang, T. Gavin, A. P. DeCaprio, R. M. LoPachin, *Toxicol. Sci.* **2010**, *117*, 180 – 189.
[42] M. J. Schnermann, C. M. Beaudry, N. E. Genung, S. M. Canham, N. L. Untiedt, B. D. W. Karanikolas, C. Sutterlin, L. E. Overman, *J. Am. Chem. Soc.* **2011**, *133*, 17494 – 17503.
[43] A. F. Barrero, M. Cortés, E. A. Manzaneda, E. Cabrera, R. Chanboun, M. Lara, A. R. Rivas, *J. Nat. Prod.* **1999**, *62*, 1488 – 1491.
[44] M. A. Cuellar, L. E. Moreno, M. D. Preite, *ARKIVOC* **2003**, *10*, 169 – 177.
[45] H. Keshmiri-Neghab, B. Goliaei, *Pharm. Biol.* **2014**, *52*, 124 – 128.
[46] F. Lefranc, G. Nuzzo, N. A. Hamdy, I. Fakhr, L. Moreno, Y. Banuls, G. Van Goietsenoven, G. Villani, V. Mathieu, R. van Soest, R. Kiss, M. L. Ciavatta, *J. Nat. Prod.* **2013**, *76*, 1541 – 1547.
[47] A. Mathieum, M. Remmelink, N. D'Haene, S. Penant, J. F. Gaussin, R. Van Ginckel, F. Darro, R. Kiss, I. Salmon, *Cancer* **2004**, *101*, 1908 – 1918.
[48] V. Mathieu, C. Pirker, E. Martin de Lasalle, M. Vernier, T. Mijatovic, N. De Neve, J. F. Gaussin, M. Dehoux, F. Lefranc, W. Berger, R. Kiss, *J. Cell. Mol. Med.* **2009**, *13*, 3960 – 3972.
[49] L. V. Frolova, I. V. Magedov, A. E. Romero, M. Karki, I. Otero, K. Hayden, N. M. Evdokimov, L. M. Y. Banuls, S. K. Rastogi, W. R. Smith, S. L. Lu, R. Kiss, C. B. Shuster, E. Hamel, T. Betancourt, S. Rogelj, A. Kornienko, *J. Med. Chem.* **2013**, *56*, 6886 – 6900.
[50] A. V. Aksenov, A. N. Smirnov, I. V. Magedov, M. R. Reisenaur, N. A. Aksenov, I. V. Aksenova, G. Nguyen, R. K. Johnston, M. Rubin, R. Kiss, V. Mathieu, F. Lefranc, J. Correa, D. A. Cavazos, A. J. Brenner, S. Rogelj, A. Kornienko, L. V. Frolova, *J. Med. Chem.* **2015**, *58*, 2206 – 2220.
[51] M. Saraswathy, S. Q. Gong, *Biotechnol. Adv.* **2013**, *31*, 1397 – 1407.
[52] G. K. Chen, G. E. Duran, A. Mangili, *Br. J. Cancer* **2000**, *83*, 892 – 898.

[53] R. Geney, M. Ungureanu, D. Li, I. Ojima, *Clin. Chem. Lab. Med.* **2002**, *40*, 918 – 925.
[54] W. G. Harker, B. I. Sikic, *Cancer Res.* **1985**, *45*, 4091 – 4096.
[55] S. K. Singh, C. Hawkins, I. D. Clarke, J. A. Squire, J. Bayani, T. Hide, R. M. Henkelman, M. D. Cusimano, B. P. Dirks, *Nature* **2004**, *432*, 396 – 401.
[56] X. Yuan, J. Curtin, Y. Xiong, G. Liu, S. Waschsmann-Hogiu, K. L. Black, J. S. Yu, *Oncogene* **2004**, *23*, 9392 – 9400.
[57] R. Galli, E. Binda, U. Orfanelli, B. Cipelletti, A. Gritti, S. De Vitis, R. Fiocco, C. Foroni, F. Dimeco, A. Vescovi, *Cancer Res.* **2004**, *64*, 7011 – 7021.
[58] J. Lee, S. Kotliarova, Y. Kotliarov, A. Li, Q. Su, N. M. Donin, S. Pastorino, B. W. Purow, N. Christopher, W. Zhang, J. K. Park, H. A. Fine, *Cancer Cell* **2006**, *9*, 391 – 403.
[59] S. Bao, Q. Wu, R. E. McLendon, Y. Hao, Q. Shi, A. B. Hjelmeland, M. W. Dewhirst, D. D. Bigner, J. M. Rich, *Nature* **2006**, *444*, 756 – 760.
[60] G. Liu, X. Yuan, Z. Zeng, P. Tunici, H. Ng, I. R. Abdulkadir, L. Lu, D. Irvin, K. L. Black, J. S. Yu, *Mol. Cancer* **2006**, *5*, 67.
[61] T. C. Johannessen, R. Bjerkvig, B. B. Tysnes, *Cancer Treat. Rev.* **2008**, *34*, 558 – 567.
[62] S. Ma, T. K. Lee, B. J. Zheng, K. W. Chan, X. Y. Guan, *Oncogene* **2008**, *27*, 1749 – 1758.
[63] S. Purkait, P. Jha, M. C. Sharma, V. Suri, M. Sharma, S. S. Kale, C. Sarkar, *Neuropathology* **2013**, *33*, 405 – 412.
[64] H. K. Gan, A. H. Kaye, R. B. Luwor, *J. Clin. Neurosci.* **2009**, *16*, 748 – 754.
[65] P. Guo, B. Hu, W. Gu, L. Xu, D. Wang, H. J. S. Huang, W. K. Cavenee, S. C. Cheng, *Am. J. Pathol.* **2003**, *162*, 1083 – 1093.
[66] A. Ligresti, A. S. Moriello, K. Starowicz, I. Matias, S. Pisanti, L. De Petrocellis, C. Laezza, G. Portella, M. Bifulco, V. Di Marzo, *J. Pharmacol. Exp. Ther.* **2006**, *318*, 1375 – 1387.
[67] C. A. Reilly, J. L. Taylor, D. L. Lanza, B. A. Carr, D. J. Crouch, G. S. Yost, *Toxicol. Sci.* **2003**, *73*, 170 – 181.
[68] R. Sancho, L. de La Vega, G. Appendino, V. Di Marzo, A. Macho, E. Munoz, *Br. J. Pharmacol.* **2003**, *140*, 1035 – 1044.
[69] E. Cao, M. Liao, D. Cheng, D. Julius, *Nature* **2013**, *504*, 113 – 118.
[70] M. H. Potashman, M. E. Duggan, *J. Med. Chem.* **2009**, *52*, 1231 – 1246.
[71] J. G. Robertson, *Biochemistry* **2005**, *44*, 5561 – 5571.
[72] J. Singh, R. C. Petter, T. A. Baillie, A. Whitty, *Nat. Rev. Drug Discovery* **2011**, *10*, 307 – 317.
[73] E. L. Kwak, R. Sordella, D. W. Bell, N. Godin-Heymann, R. A. Okimoto, B. W. Brannigan, P. L. Harris, D. R. Driscoll, P. Fidias, T. J. Lynch, S. K. Rabindran, J. P. McGinnis, A. Wissner, S. V. Sharma, K. J. Isselbacher, J. Settleman, D. A. Haber, *Proc. Natl. Acad. Sci. USA* **2005**, *102*, 7665 – 7670.
[74] W. Pao, V. A. Miller, K. A. Politi, G. J. Riely, R. Somwar, M. F. Zakowski, M. J. Kris, H. Varmus, *PLoS Med.* **2005**, *2*, 225 – 235.
[75] T. A. Carter, L. M. Wodicka, N. P. Shah, A. M. Velasco, M. A. Fabian, D. K. Treiber, Z. V. Milanov, C. E. Atteridge, W. H. Biggs, P. T. Edeen, M. Floyd, J. M. Ford, R. M. Grotzfeld, S. Herrgard, D. E. Insko, S. A. Mehta, H. K. Patel, W. Pao, C. L. Sawyers, H. Varmus, P. P. Zarrinkar, D. J. Lockhart, *Proc. Natl. Acad. Sci. USA* **2005**, *102*, 11011 – 11016.
[76] R. Dasari, L. M. Y. Banuls, M. Masi, S. C. Pelly, V. Mathieu, I. R. Green, W. A. L. van Otterlo, A. Evidente, R. Kiss, A. Kornienko, *Bioorg. Med. Chem. Lett.* **2014**, *24*, 923 – 927.
[77] R. Dasari, A. Kornienko, *Chem. Heterocycl. Compd.* **2014**, *50*, 139 – 144.
[78] R. Scott, M. Karki, M. R. Reisenauer, R. Rodrigues, R. Dasari, W. R. Smith, S. C. Pelly, W. A. L. van Otterlo, C. B. Shuster, S. Rogelj, I. V. Magedov, L. V. Frolova, A. Kornienko, *ChemMedChem* **2014**, *9*, 1428 – 1435.
[79] A. Szallasi, T. Biro, S. Modarres, L. Garlaschelli, M. Petersen, A. Klusch, G. Vidari, M. Jonassohn, S. De Rosa, O. Sterner, P. M. Blumberg, J. E. Krause, *Eur. J. Pharmacol.* **1998**, *356*, 81 – 89.
[80] M. F. Rossato, G. Trevisan, C. I. Walker, J. Z. Klafke, A. P. de Oliveira, J. G. Villarinho, R. B. Zanon, L. F. Royes, M. L. Athayde, M. V. Gomez, J. Ferreira, *Biochem Pharmacol.* **2011**, *81*, 544 – 551.

Received: August 9, 2015
Published online on October 5, 2015